Hindawi
International Journal of Energy Research
Volume 2023, Article ID 1363145, 8 pages
https://doi.org/10.1155/2023/1363145

Research Article

Study on Monitoring Reservoir Gas Density by Pulsed Neutron Logging

Guangyao Chen,[1] Lixia Dang,[2] Wenyuan Cai,[3] Jian Li,[3] Junjie Dong,[1] Zhanglong Chen,[3] and Rui Deng[1]

[1]*Key Laboratory of Oil and Gas Resources and Exploration Technology of Ministry of Education, Yangtze University, Wuhan, 430100 Hubei, China*
[2]*Yangtze University, Jingzhou, 434000 Hubei, China*
[3]*CNPC Logging Company Limited, Xian, 710077 Shaanxi, China*

Correspondence should be addressed to Lixia Dang; dlx@yangtzeu.edu.cn and Rui Deng; dengrui@yangtzeu.edu.cn

Received 27 September 2022; Revised 8 November 2022; Accepted 17 November 2022; Published 3 February 2023

Academic Editor: Weijie Yang

In mature multilayer gas reservoirs, it is a common problem to evaluate whether a potential reservoir is still productive after casing. Monitoring of unproduced or developing gas formations can guide production action plans. Intervention in unperforated zones with high gas density can increase gas production, whereas intervention in zones with low gas density is uneconomical. An RPM instrument stratum model was established by using the Monte Carlo method in this study. The model was used to simulate the response characteristics of pulsed neutron logging in a sandstone reservoir with 100% gas saturation to different reservoir gas densities, formation porosity, and shale content. The data obtained from the simulation were interpolated to construct a capture gamma ratio plate and a nonbounce gamma ratio plate. Using the constructed chart, the gas density of the reservoir can be quantitatively calculated, and then, the recovery value of the potential gas layer can be evaluated.

1. Introduction

In mature multilayer gas reservoirs, it is a common problem how to evaluate whether the undeveloped potential gas layers determined by open-hole logging still have production value after casing [1]. Intervention in unperforated zones with high gas density can increase gas production, whereas intervention in zones with low gas density is uneconomical [2]. Pulsed neutron logging technology has been widely used in the monitoring of reservoir parameters in cased wells [3–5]. However, since natural sources and neutron sources can cause irreparable damage to the human body, it is more and more common to use the MCNP program to simulate and study the problem of particle transport in the nuclear field [6, 7]. Monte Carlo method is based on probability and statistics theory, and it mainly applies random sampling method [8]. The correctness of the results can be ensured by increasing the sampling times. MCNP program can be used to calculate the photon, electron, neutron, and their mutual coupling relationship [9]. The effects of nuclear radiation encountered in practical problems can be better resolved when simulating the nuclear physics reaction process under actual conditions, and the results obtained are very reliable. The development of the pulsed neutron logging tool began in June 1963 with the successful testing of the Lane Wells' neutron lifetime logging tool [10]. In 2007, Huang et al. used the count rate ratio method of long and short source distances when studying pulsed neutron capture logging to obtain gas saturation in low-salinity water formations [11]. In 2017, Zhou et al. introduced Monte Carlo model digital processing technology to correct the influence of complex measurement environment and studied the application of RPM-C Gasview reservoir evaluation technology in Tarim oil field [12]. In 2019, Gray et al. used a combination of pulsed neutron logging data and a Monte Carlo forward modeling model to estimate the gas pressure behind the

casing and then evaluated the depletion of the condensate gas reservoir [13]. In 2020, Rose et al. studied a method for calculating reservoir gas pressure using pulsed neutron logging data [1]. In 2021, Dong et al. conducted gas layer identification research through the capture mode of pulsed neutron logging [14]. Pulsed neutron logging technology is increasingly mature after nearly 60 years of development, and it has good effects in the evaluation of remaining oil and gas after casing, oil-gas-water identification, water-out evaluation, monitoring of oil-water or gas-water interface changes, and cementing quality evaluation [10]. However, the research on the quantitative calculation of gas density is still relatively lacking, and in-depth and detailed research is needed. Therefore, this study intends to use the MCNP program to simulate the response characteristics of pulse neutron logging tool RPM to reservoir gas density, formation porosity, shale content, and other factors when gas saturation is 100%, in order to provide a basis for reservoir development potential evaluation and gas reservoir dynamic monitoring [15].

2. Principle of Measurement

The RPM pulse neutron logging tool uses the fast neutrons emitted by the pulse neutron generator to pass through the completion string to have a nuclear reaction with the formation nuclei. The receiving crystal of the tool records the gamma rays generated by the nuclear reaction, thereby detecting formation information [16, 17]. The neutron nuclear reaction in pulsed neutron logging is divided into activation reaction, inelastic scattering, elastic scattering, and capture reaction according to the level of neutron energy [18]. Activation reaction is mainly used in water velocity measurement. And reservoir gas density measurement mainly applies inelastic scattering, elastic scattering, and neutron capture.

In the inelastic scattering reaction, fast neutrons are absorbed by the target nucleus to form a renucleation, and then, a lower energy neutron is released. At this time, the target nucleus is in an excited state, and these excited nuclei often return to the ground state by emitting gamma rays. The total kinetic energy of this process is not conserved, so it is called inelastic scattering, and the resulting gamma rays are called inelastic scattering gamma rays. Besides, inelastic scattering can occur only when the energy of the incident neutron is greater than the first excited energy level of the target nucleus. In the elastic scattering reaction between fast neutrons and formation elements, the total kinetic energy of the system remains unchanged after the neutron collides with the nucleus, and all the energy lost by neutrons is converted to the kinetic energy of the recoil nucleus. No gamma rays are generated in this process. Moreover, the energy of incident neutrons is generally lower than the energy of the first excitation level of the target nucleus. In addition, the hydrogen nucleus has the greatest deceleration capacity because it loses the most energy when the neutron collides directly with the hydrogen nucleus. Fast neutrons are decelerated to become thermal neutrons and then undergo a capture reaction and neutron activation reaction with the nucleus of the atom. At this time, the target nucleus captures a thermal neutron and becomes the nucleus of the excited state. Then, the target nucleus emits one or several photons back to the ground state [19].

When the RPM logging tool is used for pulse neutron logging, the pulse frequency of the neutron generator is 1 kHz, and the pulse duration is about 60 μs including an attenuation period and pulse series composed of 28 pulses, and each attenuation period lasts 1000 μs(1 ms) [12]. The instrument probe can not actually detect elastic scattering directly because elastic scattering does not emit gamma rays. Fast neutrons will lose some energy after elastic scattering with different nuclei. Among them, hydrogen nucleus is most prone to elastic collision with neutrons, and the energy loss of neutrons in this process is very high. The hydrogen nucleus consumes the highest energy of neutrons among all atomic nuclei. Therefore, after a few times of elastic scattering between high-energy neutrons and hydrogen nuclei, the neutron energy is reduced to the extent that it is difficult to have inelastic scattering reaction with nuclei in the stratum. After several times of elastic scattering within a short distance, neutrons become thermal neutrons and are captured by surrounding nuclei. It can be approximated that the main controlling factor of the fast neutron energy loss caused by elastic scattering is the hydrogen index along the propagation path. The less energy attenuation of neutrons during the propagation process, the more likely it is to have inelastic scattering or capture reactions with the nuclei farther away from the emission source and release inelastic scattering gamma rays or capture gamma rays. Then, the ultralong source distance gamma ray probe can receive more gamma rays.

In the statistics, if the gamma rays received within the first 100 μs are selected, a R_{IN} curve can be obtained, which reflects the degree of ray attenuation controlled by inelastic scattering [12].

$$R_{\mathrm{IN}} = \frac{\int_0^{100} N_{\mathrm{SS}}(t)dt}{\int_0^{100} N_{\mathrm{XLS}}(t)dt} \approx \frac{\sum_{i=1}^{10} N_{i,\mathrm{SS}}}{\sum_{i=1}^{10} N_{i,\mathrm{XLS}}}. \quad (1)$$

In the formula, R_{IN} represents the ratio of the inelastic count rates of the near probe and the ultrafar probe, and N_{SS} and N_{XLS} are the count rates of the near and ultrafar probes, respectively. The calculation of the inelastic count rate ratio of the near probe to the far probe and the inelastic count ratio of the far probe to the ultrafar probe is similar to the above formula.

The gamma ray count rate in the later time window can also be selected in the statistical data, and the R_{capture} curve can be obtained, which can reflect the degree of ray attenuation controlled by the capture reaction.

$$R_{\mathrm{capture}} = 4 \times \frac{\int_{200}^{400} N_{\mathrm{SS}}(t)dt}{\int_{200}^{400} N_{\mathrm{XLS}}(t)dt} \approx \frac{(1/20)\sum_{i=21}^{40} N_{i,\mathrm{SS}}}{(1/80)\sum_{i=21}^{100} N_{i,\mathrm{XLS}}}. \quad (2)$$

In the formula, R_{capture} represents the ratio of the capture count rates of the near probe and the ultrafar probe, and N_{SS}

and N_{XLS} are the count rates of the near and ultrafar probes, respectively. The calculation of the capture count rate ratio of the near probe to the far probe and the capture count ratio of the far probe to the ultrafar probe is similar to the above formula.

3. RPM-MCNP Model

Since natural and neutron sources can cause irreparable damage to the human body, MCNP programs are increasingly used in the simulation of particle transport problems in the nuclear field [6, 7]. Considering wellbore size, wellbore fluid, casing size, cement ring thickness, formation porosity, reservoir gas density, mud content, and other influencing factors, pulse neutron logging was simulated. MCNP program was used to establish the basic model as shown in Figure 1. The detector source distances were 30 cm, 64 cm, and 124 cm, respectively. This model can well reflect the real situation of the stratum [20].

The specific geometric and physical parameters of the model are as follows [21]:

Stratum: the lithology is sandstone, the height is 300 cm, and the radial thickness is 150 cm.

Wellbore fluid: methane gas, 5.5 in in diameter and 300 cm in height.

Casing: the material is carbon steel, the density is 7.86 g/cm^3, the inner diameter is 5.5 in, and the thickness is 0.9 cm.

Cement ring: $CaSiO_3$ simulation, density is 1.95 g/cm^3, filled between casing and wellbore, thickness is 3 cm, and height is 200 cm.

Instrument shell: the material is 17-4PH steel, the thickness is 0.5 cm, and the height is 150 cm.

Shield: the material is B_4C.

Detector: He3 detector with high sensitivity to neutrons, regardless of the response characteristics of the detector.

Pulsed neutron source: it is located on the central axis of the logging tool, uniformly generates isotropic high-energy fast neutrons with an energy of 14 MeV, and the emission frequency of fast neutrons is 1 kHz.

On the basis of RPM instrument formation model, MCNP program is used to simulate the response characteristics of RPM instrument under different formation conditions, and the response relationship of pulse neutron logging to gas density change in reservoir is analyzed, so as to find a quantitative method to detect gas density change, which provides theoretical basis for the actual production of gas fields.

4. Gas Layer Response Law

Using RPM instrument formation model, considering the actual situation during mining, the wellbore is filled with gas, the formation lithology is set to quartz sandstone, and the gas saturation is 100%; the gas density is set to 0.2, 0.3, 0.4, 0.5, 0.6, 0.7, 0.8, 0.9, and 1.0 g/cm^3, respectively, and the formation porosity is 0%, 5%, 10%, 15%, 20%, 25%, 30%, and 35%, respectively. The capture gamma count rate and inelastic gamma count rate of the near, far, and ultrafar probes are simulated, and these data are processed and analyzed to obtain the gas layer response law.

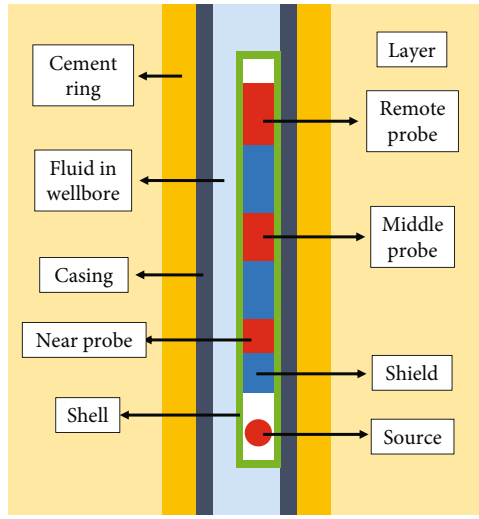

Figure 1: RPM instrument formation model.

4.1. Sensitivity Analysis of Combination Probes. In order to analyze which of the three probe combinations of near-far, near-ultrafar, and far-ultrafar is more sensitive to the change of the hydrogen index in the formation, the gamma ray count ratios of each combination under each density value of the gas were calculated and normalized. After comparison, it is found that the variation of gamma count rate ratio with porosity of each combination is consistent within the set gas density range. Therefore, only one gas density value is selected to display and analyze the response of each combination of gamma count rate ratios to changes in porosity.

Figure 2 shows the normalized gamma count rate ratio for each combination as a function of formation porosity at a gas density of 0.4 g/cm^3. In the figure, R^* is the normalized gamma count rate ratio, and "1-2", "1-3", and "2-3" represent the combination of near-far, near-ultrafar, and far-ultrafar probes, respectively. By comparison, it is found that the combination of near-ultradistant probes is most sensitive to the change of the hydrogen index in the formation, so the ratio of the count rate of the near and ultradistant probes can better reflect the response characteristics of gas density changes in the reservoir.

4.2. Law of Capture Response of Gas Layer. Select the capture gamma count rate data of the near probe and the ultradistant probe and use the ratio of the capture count rate of the near probe to the capture count rate of the ultradistant probe to obtain the response relationship between the ratio of the capture count rate of the near-ultradistant probe and the gas density under different formation porosity conditions.

It can be seen from Figure 3 that the capture gamma count ratio of the near and ultrafar probes increases significantly with the increase of gas density when the formation porosity is constant. As formation porosity increases, $R_{capture}$ becomes more responsive to gas density changes. At a constant gas density, $R_{capture}$ increases as formation

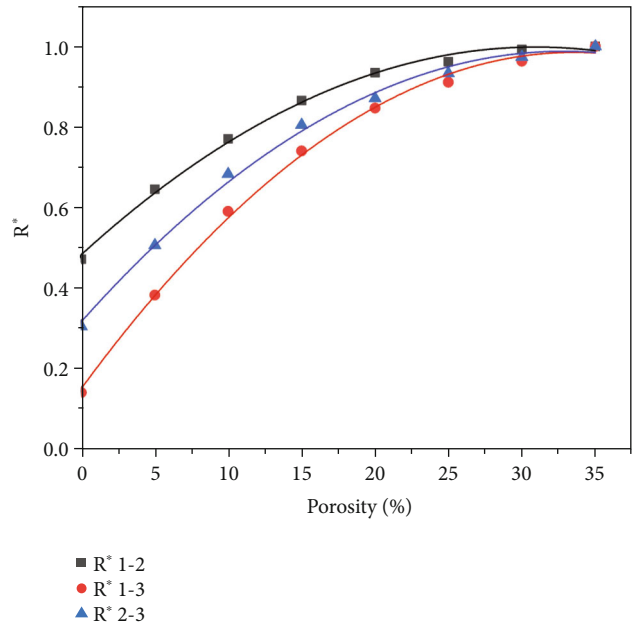

Figure 2: RPM probe gamma count rate ratio sensitivity comparison.

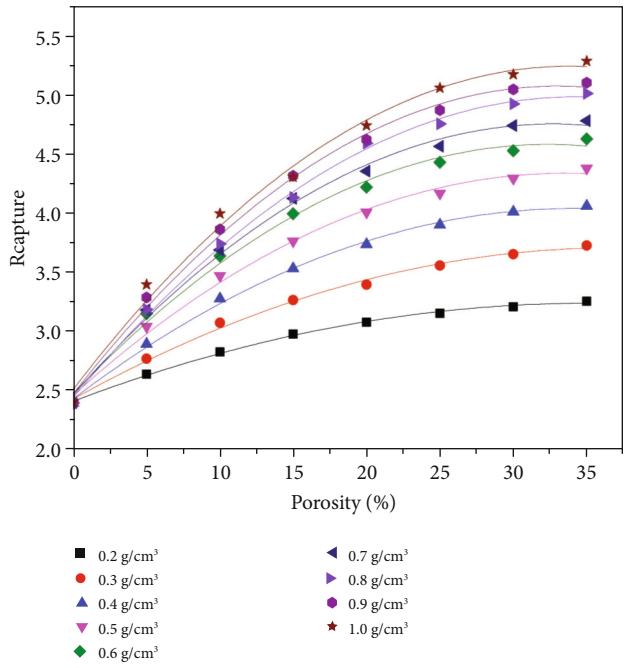

Figure 3: Response law of capture gamma count ratio under different porosity conditions.

porosity increases. As gas density increases, $R_{capture}$ becomes more responsive to porosity changes.

4.3. Inelastic Response Law of the Gas Layer. Select the inelastic gamma count rate data of the near probe and the ultradistant probe and use the ratio of the inelastic count rate of the near probe to the inelastic count rate of the ultradistant probe to obtain the response relationship between the ratio of the inelastic count rate of the near-ultradistant probe and the gas density under different formation porosity conditions.

It can be seen from Figure 4 that in the case of a certain formation porosity, the nonelastic gamma count ratio of the near and ultrafar probes increased significantly with the increase of gas density, and the greater the porosity, the more obvious the response of R_{IN} to the change of gas density. At a constant gas density, R_{IN} decreases with increasing porosity if the gas density is less than or equal to 0.6 g/cm^3, and R_{IN} increases with increasing porosity if the gas density is in the range of 0.7 to 1.0 g/cm^3.

In neutron logging, the hydrogen content of fresh water is defined as a unit, and the ratio of the number of hydrogen nuclei in any rock or mineral 1 cm^3 to the number of hydrogen nuclei in the same volume of fresh water is defined as its hydrogen index. The hydrogen index is represented by H. It is proportional to the number of hydrogen nuclei in the medium per unit volume. For fresh water, there are

$$H = k\frac{N_A x\rho}{M}. \tag{3}$$

In the above formula, M represents the molar mass of the compound, ρ represents the density, x represents the number of hydrogen atoms in each molecule of the compound, and k represents the undetermined coefficient.

Fresh water is given a hydrogen index of 1, so that the hydrogen index of a mineral or rock composed of a compound can be determined by the following formula:

$$H = 9 \times \frac{x\rho}{M}. \tag{4}$$

The hydrogen concentration of natural gas (molecular formula is nCH_x) is very low and changes with density, and its hydrogen index is

$$H = 9\frac{nx\rho}{n(12+x)} = 9\frac{x}{12+x}\rho. \tag{5}$$

From nCH_x, the hydrogen index of methane (CH_4) is

$$H_{CH_4} = 2.25\rho_{CH_4}. \tag{6}$$

It can be seen from the above formula that the hydrogen index of methane is proportional to its density. When the gas density is small, the hydrogen index of the gas is low, and the deceleration ability of the same volume gas is weaker than that of the stratum with the same volume. At this time, when the gas density is fixed, the deceleration ability of the stratum decreases with the increase of porosity. As the density of the gas increases, the hydrogen index of the gas gradually increases. When the gas density is greater than or equal to 0.7 g/cm^3, the deceleration ability of the same volume of gas is stronger than that of the same volume of formation. In this case, when the gas density is fixed, the deceleration ability of the formation increases with the increase of porosity. This also confirmed the rationality of

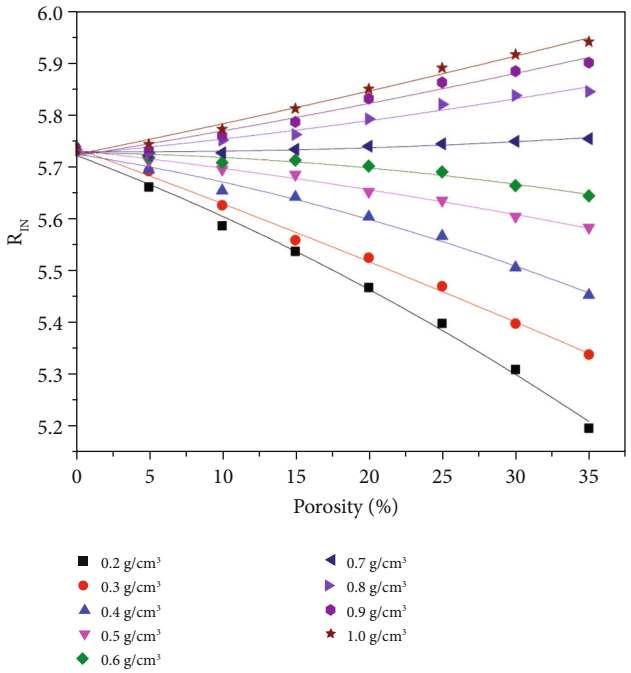

Figure 4: Response law of nonelastic gamma count ratio under different porosity conditions.

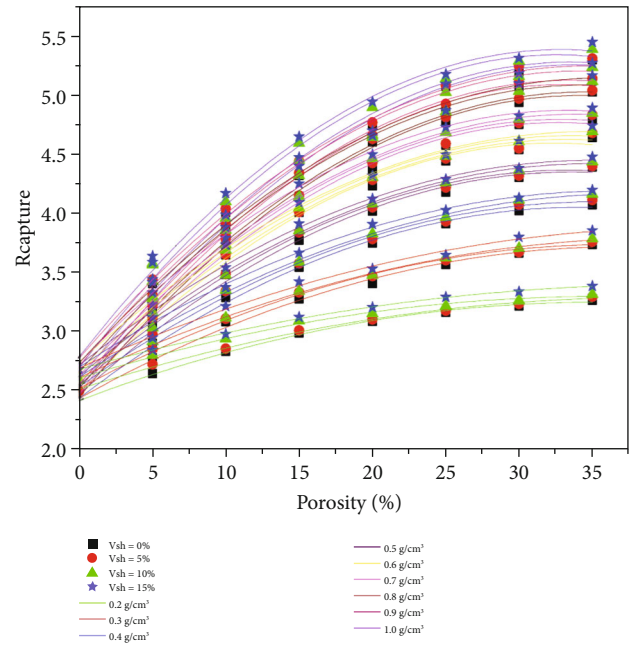

Figure 5: Effect of shale content on the ratio of capture gamma counts.

R_{IN}'s different response with formation porosity under different gas density conditions.

5. Influence of Shale Content on Gas Layer Response

Using the same calculation model, the diameter of the wellbore is 20 cm, the wellbore is filled with gas, the formation lithology is set to quartz sandstone, the gas saturation is 100%, and the shale content in the formation is set to 0%, 5%, 10%, and 15%, respectively; the gas densities are 0.2, 0.3, 0.4, 0.5, 0.6, 0.7, 0.8, 0.9, and 1.0 g/cm^3, respectively, and the formation porosity is 0%, 5%, 10%, 15%, 20%, 25%, 30%, and 35%, respectively. By simulating the capture and inelastic counts of the combination of near and ultrafar detectors, the response relationship between the ratio of the capture count rate and the gas density and formation porosity, and the response relationship between the ratio of the inelastic count rate and the gas density and formation porosity under the condition of different shale contents in the formation are obtained.

5.1. Effect of Shale Content on the Ratio of Capture Gamma Counts. From the data distribution in Figure 5, the increase of porosity makes the $R_{capture}$ gap between different gas densities larger; that is, with the increase of porosity, the ability of $R_{capture}$ to identify the gas density increases. Its specific manifestation is that with the increase of gas density, the response curve gradually moves up and presents the characteristics of layered display. When the formation porosity is constant, $R_{capture}$ increases significantly with the increase of gas density. The influence of shale content on this value is that no matter what the gas density is, the increase of shale content will cause a slight increase in $R_{capture}$, and when the gas density is constant, regardless of the formation porosity, the increase of shale content will cause a slight increase in $R_{capture}$. The results show that the influence of shale content cannot be ignored when using $R_{capture}$ to quantitatively study the gas density, and the influence of shale content must be taken into account.

5.2. Effect of Shale Content on Gamma Count Ratio of Inelastic Scattering. From the data distribution in Figure 6, the increase of porosity makes the R_{IN} gap between different gas densities larger; that is, with the increase of porosity, the ability of R_{IN} to identify the gas density increases. Its specific manifestation is that with the increase of gas density, the response curve gradually moves up and presents the characteristics of layered display. When the formation porosity is constant, R_{IN} increases significantly with the increase of gas density. The influence of shale content on this value is that no matter what the gas density is, the increase of shale content will cause a slight increase in R_{IN}, and when the gas density is constant, regardless of the formation porosity, the increase of shale content will cause a slight increase in R_{IN}. The results show that the influence of shale content cannot be ignored when using R_{IN} to quantitatively study the gas density, and the influence of shale content must be taken into account.

6. Interpolation and Gamma Count Ratio Maps

Although the capture gamma count ratio and the inelastic gamma count ratio of many sample points were obtained through MCNP simulation, these discrete data are not enough for quantitative interpretation of the gas density in

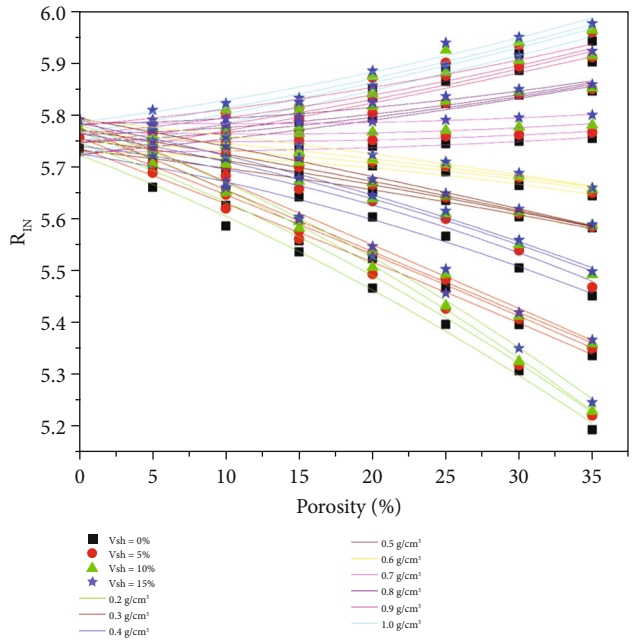

Figure 6: Effect of shale content on gamma count ratio of inelastic scattering.

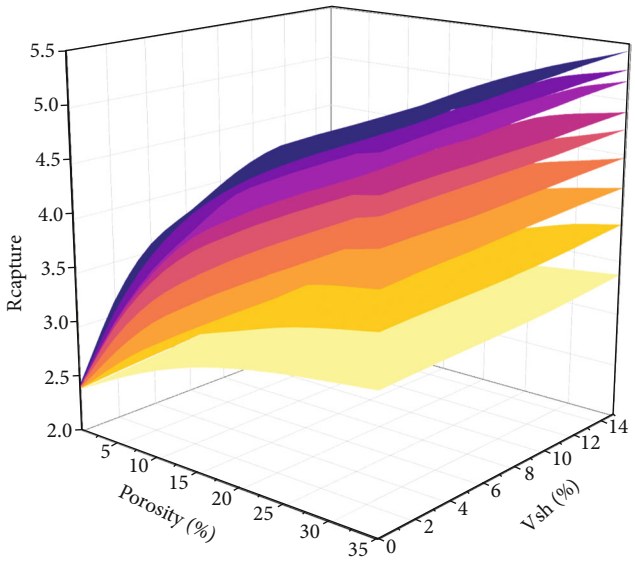

Figure 7: Capture gamma ratio plate.

the gas layer, and the interpolation method can be used to solve this problem well [22]. Interpolation is the most basic operation method in numerical analysis. It uses the function value of the function $f(x, y)$ at several known points in a certain interval to make an appropriate specific function and uses the value of the specific function at other points in the interval as the approximate value of the function $f(x, y)$.

Through the above research, it can be seen that the capture gamma count rate ratio R_{capture} and the inelastic scattering gamma count rate ratio R_{IN} of the near probe and the ultrafar probe have a significant relationship with

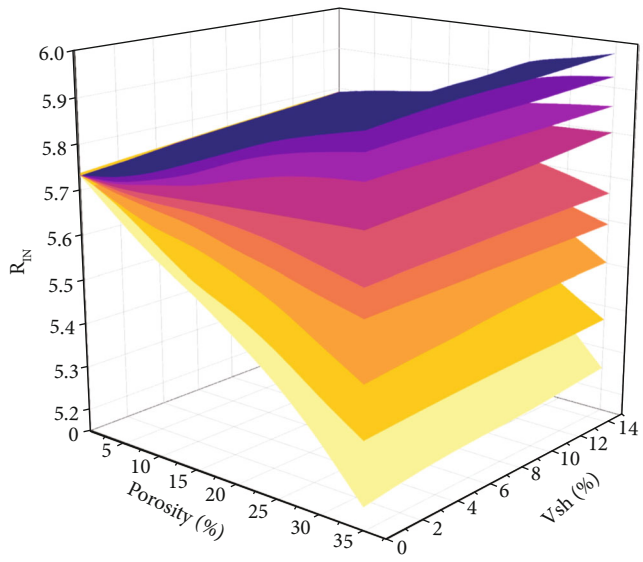

Figure 8: Inelastic scattering gamma ratio plate.

the formation porosity, reservoir gas density, and shale content. Using interpolation method to process the existing data, a capture gamma ratio chart and an inelastic scattering gamma ratio chart are made (Figures 7 and 8). In the charts, R_{capture} and R_{IN} have a one-to-one correspondence with formation porosity, reservoir gas density, and shale content. Thereby, the purpose of calculating reservoir gas density can be achieved through formation porosity, shale content, R_{capture}, or R_{IN}.

7. Conclusion

Currently, the RPM logging tools used in various oil fields usually have three gamma-ray detectors with different source distances, and the capture and inelastic scattering gamma count rates received by different detectors can reflect the different strata information. In this study, the Monte Carlo method and the MCNP program were used to establish an RPM-stratigraphic model to simulate the response of the RPM tool in a sandstone reservoir with 100% gas saturation. Different formation porosity, reservoir gas density, and shale content were set in the simulation, and their influence on pulsed neutron logging was deeply explored, and the following conclusions were obtained:

(1) According to the sensitivity analysis of the combined detectors, it is found that the ratio of the gamma count rate of the near probe and the ultrafar probe is more sensitive to the change of the formation hydrogen index

(2) Methane gas has a mutation point in the density value. When the methane density value is at this point, the hydrogen index of the same volume of methane is equal to the hydrogen index of the same volume of reservoir. Under the research conditions

set in this study, the mutation point is between 0.6 g/cm^3 and 0.7 g/cm^3

(3) Formation porosity, reservoir gas density, and shale content have obvious effects on capture gamma count rate ratio $R_{capture}$ and inelastic scattering gamma count rate ratio R_{IN}. Through the relationship between them, the capture gamma ratio plate and the inelastic scattering gamma ratio plate can be constructed. Using the constructed plates, the reservoir gas density can be calculated from the formation porosity, shale content, $R_{capture}$, or R_{IN}

(4) Due to the lack of actual measurement data of gas density in the gas layer, it is impossible to combine the simulation results with the actual data. Therefore, the research results of this paper only provide a new idea for gas density monitoring research

Data Availability

The data that support the findings of this study are available on request from the corresponding author (RD).

Conflicts of Interest

The authors declare that they have no known competing financial interests or personal relationships that could have appeared to influence the work reported in this paper.

Authors' Contributions

Guangyao Chen and Junjie Dong were responsible for the conceptualization, data curation, methodology, investigation, validation, and writing of the original draft. Lixia Dang and Rui Deng were responsible for the supervision, formal analysis, funding acquisition, resources, and writing (review and editing). Wenyuan Cai, Jian Li, and Zhanglong Chen were responsible for the supervision, formal analysis, and resources.

Acknowledgments

The research is funded by the National Major Science and Technology Projects of China "Multidimensional and High Precision Imaging Logging Series" (No. 2017ZX05019001) and the Key Project of Science and Technology Research Program of Hubei Provincial Department of Education (grant number D20191302).

References

[1] D. Rose, A. A. Stephens, T. Zhou, L. Bolerjack, and K. Kenning, "Gas Pressure Estimation in Cased Hole Using a Pulsed Neutron Log," in *SPWLA 61st Annual Online Symposium*, 2020.

[2] C. Cavalleri, G. Brouwer, D. Kodri, D. Rose, and A. Brinks, "Maximizing the Value of Data Acquisition: Gas Pressure Assessment through Casing-A Complex Cased Hole Pulse Neutron Case Study from the Netherlands," in *SPWLA 61st Annual Online Symposium*, 2020.

[3] A. Al-Qasim, I. Mostefai, S. Kokal, and A. Alkhateeb, "Formation Evaluation Using Advanced Pulsed Neutron Tools," in *SPE Gas & Oil Technology Showcase and Conference*, Dubai, UAE, 2019.

[4] R. Brackenridge, R. Ansari, D. Chace, A. Zett, M. Webster, and D. Itter, "Evaluation of new multi-detector pulsed neutron logging techniques to monitor mature North Sea reservoir saturations," in *SPWLA 52nd Annual Logging Symposium*, Colorado Springs, Colorado, 2011.

[5] J. Liu, F. Zhang, C. Zhou et al., "Methods for Evaluating Elemental Concentration and Gas Saturation by a Three-Detector Pulsed-Neutron Well-Logging Tool," in *SPWLA 58th Annual Logging Symposium*, Oklahoma City, Oklahoma, USA, 2017.

[6] R. Ansari, N. Mekic, D. Chace, M. Rust, and M. Starr, "Field applications of a new cased hole gas saturation measurement in tight gas reservoirs," in *SPWLA 50th Annual Logging Symposium*, The Woodlands, Texas, 2009.

[7] F. Inanc, W. A. Gilchrist, and D. Chace, "Physical Basis, Modeling, And Interpretation Of A New Gas Saturation Measurement For Cased Wells," in *SPWLA 50th Annual Logging Symposium*, The Woodlands, Texas, 2009.

[8] H. K. Choi, R. P. Gardner, and K. Verghese, "Monte Carlo simulation of the neutron lifetime logging tool," *Transactions of the American Nuclear Society (United States)*, vol. 52, 1986.

[9] F. Zhang, C. Yuan, S. Hou, and X. Wang, "Numerical simulation of natural gas identification by pulsed neutron logging while drilling," *Natural Gas Industry*, vol. 30, pp. 18–21, 2010.

[10] Z. Wang and Q. Zhou, "Review of development of cased hole pulse neutron logging tools," *Well Logging Technology*, vol. 44, pp. 432–437, 2020.

[11] D. Huang, C. Song, X. Shen, Z. Huang, and H. Ma, "Research and application of a method for obtaining gas saturation in low-salinity water formations by pulsed neutron capture logging," *China Offshore Oil and Gas*, vol. 2007, no. 3, pp. 169–172, 2007.

[12] J. Zhou, L. Deng, C. Wang, Y. Fang, and H. Yu, "Application of RPM-C Gasview reservoir evaluation technology in the Tarim oilfield," *Well Logging Technology*, vol. 41, pp. 108–113, 2017.

[13] R. Gray, E. Smith, A. Parsa, Y. Kim, and G. Odusi, "Identification of Remaining Reserves Using Pulsed Neutron Logging for Pressure Determination behind Casing in Mature Gas Condensate Reservoirs," in *SPE Annual Technical Conference and Exhibition*, Calgary, Alberta, Canada, 2019.

[14] J. Dong, R. Deng, Z. Quanying, J. Cai, Y. Ding, and M. Li, "Research on recognition of gas saturation in sandstone reservoir based on capture mode," *Applied Radiation and Isotopes*, vol. 178, article 109939, 2021.

[15] R. Nardiello, Y. Kim, D. Chace et al., "Cased Hole Reservoir Pressure Analysis Using Pulsed Neutron Log Measurements in Challenging Mature Environments-Physics, Modeling, Uncertainty Assessment and Application," in *SPWLA 58th Annual Logging Symposium*, Oklahoma City, Oklahoma, USA, 2017.

[16] L. Jacobson, D. Durbin, and S. Reed, "An Improved Formation Density Measurement Using PNC Tools," in *SPE Annual Technical Conference and Exhibition*, Houston, Texas, 2004.

[17] C. W. Morris, J. F. Vaeth, and D. J. Verret, "Differentiation of gas in sand/shale environments using pulsed neutron capture measurements. Oil field," in *SPE Annual Technical Conference and Exhibition*, San Antonio, Texas, 1997.

[18] T. Zhou, D. Rose, T. Quinlan et al., "Fast Neutron Cross-Section Measurement Physics and Applications," in *SPWLA 57th Annual Logging Symposium*, Reykjavik, Iceland, 2016.

[19] F. Zhang, *Fundamentals of Nuclear Geophysics*, Petroleum Industry Press, 2015.

[20] N. Mekic, C. Mcilroy, F. Hill, and W. Guo, "Multidetector Pulsed-Neutron Technology for Low-Porosity Reservoir-Interpretation Methodology," in *SPWLA 57th Annual Logging Symposium*, Reykjavik, Iceland, 2016.

[21] Z. Wang, B. Tang, X. Xiang, and D. Wu, "Research on RPM log interpretation simulation method for offshore heavy oil reservoirs," *Chinese Journal of Engineering Geophysics*, vol. 13, pp. 405–410, 2016.

[22] V. I. Aronov, "A method for 3-D interpolation and modeling of geophysical and geological scattered data," *SEG Technical Program Expanded Abstracts*, vol. 14, p. 1566, 1995.